

Bio-organism sensing via surface enhanced Raman spectroscopy on controlled metal/polymer nanostructured substrates

M. C. Demirel^{a)}

Materials Research Institute and Department of Engineering Science, The Pennsylvania State University, University Park, Pennsylvania 16802

P. Kao

Department of Chemistry, The Pennsylvania State University, University Park, Pennsylvania 16802

N. Malvadkar and H. Wang

Department of Engineering Science, The Pennsylvania State University, University Park, Pennsylvania 16802

X. Gong and M. Poss

Department of Biology and Center for Infectious Disease Dynamics, The Pennsylvania State University, University Park, Pennsylvania 16802

D. L. Allara^{a)}

Materials Research Institute and Department of Chemistry, The Pennsylvania State University, University Park, Pennsylvania 16802

(Received 20 March 2009; accepted 8 May 2009; published 4 June 2009)

A new class of nonlithographically prepared surface enhanced Raman spectroscopy (SERS) substrates based on metalized, nanostructured poly(*p*-xylylene) films has been developed and optimized for surface plasmon response with a view to applications of SERS detection of microbial pathogens, specifically, bacteria and viruses. The main emphasis has been on achieving high spot to spot, sample to sample reproducibility of the SERS signals while maintaining useful enhancement factors. The use of these surfaces, metalized with either Ag or Au, provides a noninvasive and nondestructive method for spectral fingerprint analyses of both bacteria and viruses. Examples are given for the detection of bacteria (*E. coli* and *B. cereus*) and viruses (respiratory syncytial virus and Cocksackievirus). Our method is able to distinguish Gram positive from Gram negative bacterial strains as well as enveloped and nonenveloped viruses. The results demonstrate the development of a new class of SERS substrates which can provide rapid, selective identification of infectious agents without amplification of cultures. © 2009 American Vacuum Society. [DOI: 10.1116/1.3147962]

I. INTRODUCTION

Nanotechnology is being increasingly viewed as offering new ways to generate technological advancements in a variety of areas. One of the critical areas of potential benefit is diagnostic microbiology where the central problem of sensing and detecting microbial pathogens suffers from a general lack of rapid, economical detection methods.¹ For any pathogen detection method to be successful three major barriers must be overcome: (1) sensitivity, (2) reproducibility, and (3) selectivity. One technique that offers a potential solution is surface enhanced Raman spectroscopy (SERS).^{2,3} Raman spectroscopy, in general, offers advantages for analyzing biological molecules due to its abilities to provide *in situ* analyses directly in aqueous systems⁴ and the inherent fingerprint characteristics of the spectra formed by the unique molecular vibrations of each specific analyte molecule. This approach can avoid the typical, more laborious methods involving reagents and amplification of cultures. Raman spectroscopy, however, suffers greatly from the problem of sensitivity. Only bulk samples of the analyte of interest or reasonably

concentrated solutions can give sufficient signal/noise to generate useful spectra. For applications to rapid analyses of microbial pathogens it is useful to be able to collect trace amounts of the pathogens (for example, from air samples) on surfaces and then analyze directly; a challenge that cannot be met by standard Raman spectroscopy.

In contrast, in the SERS mode the Raman signal per molecule can be amplified by factors of a million or more,^{5,6} even down to the single molecule level,⁷ leading to the ability to generate useful detection signals for trace amounts of pathogens. The major feature of a SERS active surface is the presence of a metal, particularly Ag or Au, with nanoscale size features capable of sustaining surface plasmon polariton (SPP) resonances with the laser excitation used to generate the Raman signal of the analyte molecules. Typically the nanoscale features are produced by the use of nanoparticles, roughened surfaces or lithographically fabricated features,^{8–10} and can consist of combinations of sharply pointed features and gaps. As these feature sizes decrease to the limit of the atomic scale the SPP resonances are dramatically enhanced, leading to extraordinarily large local electromagnetic fields which, in turn, leads to huge magnifications of the Raman scattering signals of molecules located at the local feature (*hot spot*). The combination of the high sensi-

^{a)}Authors to whom correspondence should be addressed; electronic addresses: mdemirel@engr.psu.edu and dla3@psu.edu

tivity and the fingerprint spectral capability of SERS has led to interest in a broad variety of biomedical types of applications including rapid DNA sequencing,¹¹ pathogen detection,¹² and food analysis.¹³ Of particular interest to us has been the potential ability of SERS to obtain vibrational spectra from surface collected pathogens that could be used for detection and identification without reagents and further provides the chemical composition of pathogen membranes, which then could serve as a highly specific identification marker. There is significant interest in developing an optimum detection configuration in which a SERS sample collection surface in combination with a handheld spectrometer could provide a rapid, reagentless detection of pathogens with minimal sample preparation and ease of operation. Such a method would provide distinct advantages over typical methods using electrochemical (e.g., potentiometric and amperometric), mechanical (e.g., quartz crystal microbalance and surface acoustic), and optical (e.g., fluorescence and surface plasmon resonance) technologies.

While the SERS technique clearly is well established for achieving high sensitivity, which is of great value in facilitating rapid measurements, the two challenges of reproducibility and selectivity remain. In more detail high spot-to-spot and substrate to substrate reproducibility is needed to minimize false positives and negatives,¹⁴ of critical importance in pathogen detection. For selectivity it is important to note that whereas the SERS signals are built of fingerprint vibrational spectra emanating from molecules located at the *hot spots* the collocation (or coadsorption) of impurities and interfering background species can mask the analyte signal of interest. Thus to meet this challenge it is useful to synthesize SERS surfaces which exhibit selectivity in binding the analyte of interest to the *hot spot*. Early efforts in pathogen detection were directed primarily toward obtaining high sensitivities (enhancement factors or EFs) by creating rough silver or gold substrates using electrochemical etching,⁸ deposition of metal island films on a flat substrate⁹ or metal nanoparticles immobilized on a substrate.¹⁰ These approaches indeed produced useful EFs but have not yet led to significant advances in overcoming the major problem of poor control over the reproducibility of the SERS substrate nor has the issue of substrate selectivity been seriously addressed. Photolithography to prepare uniform SERS substrates was proposed as a solution to the reproducibility problem¹⁵ but the large feature sizes are not ideal to obtain a good EFs. Advanced lithographic and patterning techniques such as electron beam lithography,¹⁶ nanosphere lithography,¹⁷ and self-assembled monolayers to pattern a colloidal gold monolayer¹⁸ were used to prepare highly ordered SERS substrates, which presumably would lead to uniform signals across the substrates. A detailed discussion of the individual advantages and disadvantages of these methods has been published recently by Tripp *et al.*¹⁹ Complex, expensive multiple fabrication steps and/or poor sample stability under analysis conditions, however, diminish the practicality of these approaches.

Recently, with a view to overcoming these problems, we developed a new class of nonlithographically prepared SERS substrates based on vacuum deposited polymer films with highly controllable columnar nanostructures²⁰⁻²³ which were further coated with a vacuum deposited Au or Ag thin film. The novel concept was to (1) first build tunable nanomorphology substrates by varying processing conditions and the polymer materials and (2) then metalize the nanostructured surfaces by carefully selected, controlled metalization processes such that the final structure was optimized for a useful combination of EFs, reproducibility and analyte selectivity. In our first trials simple sets of preparation conditions produced SERS active characteristics and lead to significant improvements in obtaining reproducible spectral data compared to other standard types of SERS surfaces in common use for analytical applications. For example, for a Ag coated columnar nanostructured polymer substrate we are able to obtain ~5% signal variation over a 1 mm² area with ~1 μm analysis spot sizes, and similar high sample to sample reproducibility while providing a highly stable surface with the capability of sustaining the integral structure of biospecies.²⁴ In comparison, the use of comparable nanostructured Ag thin films on glass slides, a common SERS substrate, indeed provided excellent signal enhancement, as expected, but showed high irreproducibility spot to spot and sample to sample, compared to the metalized polymer films. Further the Ag/glass island films showed poor stability as a capture surface whereas the metalized polymer substrates are exceedingly stable. In this paper, we report our first findings confirming the applicability of the metalized, nanostructured polymer substrates for pathogen detection with demonstrations from examples of bacterial (*E. coli* and *B. cereus*) and viral (respiratory syncytial virus, *RSV* and *Coxsackievirus*) pathogens.

II. MATERIALS AND METHODS

A. SERS substrate preparations

Fused silica microscope slides or highly polished silicon substrates were cleaned with acetone and isopropanol prior to polymer deposition. In some cases to ensure high cleanliness, peroxy-sulfuric acid or concentrated ammonia solution with 30% H₂O₂ was used before the solvent rinses. The freshly cleaned substrate was mounted in the polymer deposition chamber and fixed in the desired tilted orientation relative to the incoming vapor. The deposition of columnar poly(chloro-*p*-xylylene) (PPX-Cl) films by oblique angle polymerization has been described in our previous work.²⁰⁻²³ Briefly, the dimer precursor dichloro-[2.2]paracyclophane was placed in a deposition cell in the vacuum chamber and fixed to allow a deposition area of ~1 cm² on the substrate. The chamber was evacuated and the precursor then converted to a reactive gas of monomers by pyrolysis (690 °C). The vapor pressure in the deposition chamber was maintained at approximately 10–20 mTorr. The deposition process was completed 10 min after the required vacuum level has been achieved. After removal from the polymer deposition chamber the sample was mounted in a cryogenically pumped

electron beam deposition chamber equipped with a Quartz Crystal Microbalance for monitoring the deposited film thickness. The metal (silver or gold) layer was deposited on the PPX-Cl films under a base pressure of $\sim 1 \times 10^{-8}$ torr with the deposition rate maintained at 7–8 Å/s. After removal the samples were stored in closed containers for no more than 1 h before use. Immediately prior to the incubation of *E. coli* or *respiratory syncytial virus* (RSV) the silver (or gold) surface was cleaned using UV ozone for 2 min.

Comparison SERS substrates using standard Ag nanoparticle islands on glass slides were prepared by vacuum deposition of Ag onto clean glass slides using identical deposition conditions as for the PPX-Cl substrates. Films of various selected thicknesses were prepared and characterized for SERS and UV-vis transmission spectra.

B. Sample characterizations

A JEOL 6700F field-emission scanning electron microscope operated at an accelerating voltage of 3 kV was used to characterize the morphology of the metalized (Ag) nanostructured PPX films. Raman spectra were obtained using a Renishaw inVia micro-Raman instrument equipped with a cooled silicon charge coupled device detector, a 0.75 numerical aperture objective lens, a 1200 lines/mm grating (1 cm^{-1} resolution) and selectable excitation at 514.5 or 632.8 nm. The spectra reported here were obtained using a 35 mW HeNe laser (632.8 nm) excitation source. The position of the sample relative to the excitation spot was moved by a motorized, software controlled microscope stage.

The motorized microscope stage allows SERS maps of the surface to be formed. The instrument parameters were 50 \times objective and 10 s acquisition time per spectrum. Electron microscope images were obtained using a Philips-420 tungsten-based transmission electron microscope (TEM) operating at 120 kV. The Cary 100 UV-vis was used to obtain absorbance data for the metalized nanostructured PPX films. Deuterium light source was used in UV/vis measurement in the 200–800 nm ranges with the spectral bandwidth set as 1 nm.

C. *E. coli*

E. coli was purchased from Lucigen (BL21-DE3) and after subculturing, single colonies were collected using sterile plastic inoculating loops and cultivated for 4 h at 37 °C on a LB agar base. 10 μl of bacteria aliquots were placed on a SERS substrate for immediate characterization.

D. *B. cereus*

B. cereus (ATCC No. 9818) was kindly provided by Doores. After subculturing, single colonies were collected using sterile plastic inoculating loops and cultivated for 4 h at 37 C on a LB agar base. Ten bacteria aliquots were placed on a SERS substrate for immediate characterization.

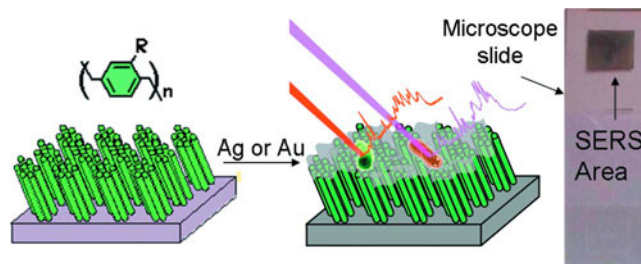


FIG. 1. (Color online) Description of SERS substrate preparation and pathogen detection: (i) Nanostructured poly(*p*-xylylene) (PPX) films are prepared using an oblique angle polymerization method, (ii) SERS-active metals (e.g., Au and Ag) are deposited onto the nanostructured PPX using. The inset shows the nanostructured SERS substrate deposited on a microscope slide.

E. Respiratory syncytial virus

The virus was produced in Hep-2 cells grown in Opti-MEM (Invitrogen) with 2% fetal bovine serum (FBS), 1% L-Glutamine, 50U/ml penicillin, and 50 $\mu\text{g}/\text{ml}$ streptomycin. Five days after inoculation, virus-containing supernatant was harvested and clarified at 3200 g for 20 min. We did not recover the virus by lysing cells to minimize contamination of particles by host nucleic acid, which is visible on the surface of particles purified by cell lysis by SERS. Supernatant was brought to 50 mM tris, pH 7.5, 0.1M MgSO_4 and precipitated at 4 °C for 90 min with moderate stirring using a final concentration of 10% PEG 6000. The precipitate, containing viral particles, was collected by centrifugation at 3200x g for 20 min. The pellet was gently resuspended in 7 ml of cold buffer consisting of 150 mM NaCl, 50 mM tris-HCl, 100 mM MgSO_4 and layered onto a discontinuous (30%, 45%, 60%) sucrose gradient. Samples were centrifuged in a Beckman SW28 rotor at 100 000x g at 4 °C for 100 min. The 2–3 ml interface between the 30% and 45% sucrose layers was collected and 1 ml aliquots were frozen for titer and subsequent use. Infectious titer was determined by plaque assay on Hep-2 cells and total virus titer was determined by quantitative PCR.

F. Coxsackievirus B3 virus

Coxsackievirus B3 strain (ATCC VR30) was kindly provided by Cameron and was used as received.

III. RESULTS AND DISCUSSION

A. Surface morphologies, optical characterization, and SERS enhancement factors

The schematic in Fig. 1 highlights the preparation of the metalized PPX-Cl films. The PPX-Cl film structure has been shown to consist of a carpet of densely packed, aligned fibers (approximately $4 \times 10^7/\text{mm}^2$).²⁵ This structure can be produced with high reproducibility and is easily varied by selecting different processing conditions. A typical size distribution of the Ag nanoparticle features is given in Fig. 2(a) for the example of a 60 nm Ag film deposited on a PPX-Cl substrate. The figure shows a histogram, constructed from

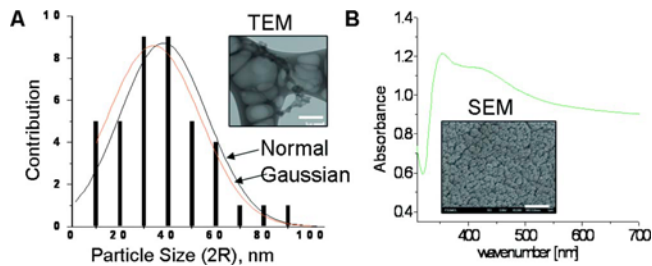


FIG. 2. (Color online) (a) Size distribution of Ag nanoparticles for a 60 nm deposited Ag film on a PPX-Cl substrate film taken from cross section TEM data; the inset shows a representative TEM image of the nanoparticles (scale bar of 100 nm). (b) Optical absorbance spectrum for the Ag film deposited on the nanostructured polymer substrate (corrected for the PPX-Cl film absorption of a slowly, monotonically increasing absorbance base line to lower wavelengths). Inset: SEM micrograph (top view) of the Ag/PPX film (the white bar in the lower right hand side represents 2 μm).

several cross section TEM images, with an average Ag particle diameter of ~ 38 nm and a standard deviation ~ 8 nm, a typical moderate size distribution width for metallic nanoparticles. The inset in Fig. 2(a) shows an example of a TEM image of the nanoparticles for the 60 nm Ag film. The optical absorbance spectra obtained from the metalized PPX-Cl film, shown in Fig. 2(b), reveals two major plasmon peaks at ~ 360 and ~ 420 nm. In general, the overall positions of the features are in good agreement with simple Mie theory²⁶ and earlier work on Ag nanoparticles.¹⁰ The peaks, respectively, can be assigned to the $n=1$ (dipole) and $n=2$ (quadrupole) modes. Thicker Ag films exhibit a reduction in intensity of the $n=2$ relative to the $n=1$ peak, corresponding to an increase in the average nanoparticle radius (data not shown). We note that the broad tail of the plasmon spectrum may be a significant and important aspect of these films, reflecting critical morphology distributions of the metal nanoparticles embedded within the polymer columnar nanostructures and further study is underway to develop this point. A scanning electron microscope (SEM) image showing the nanostructured morphology of the 60 nm Ag metalized PPX-Cl film is shown in Fig. 2(b).

The enhancement factors (EFs) for the Ag metalized substrates were estimated using the C-F stretching mode ($\nu_{\text{C-F}}$) of 4-fluorobenzenethiol (FBT) molecules that were chemisorbed in monolayer form (self-assembled monolayer) onto the metalized substrates. The EF is given by

$$\text{EF}(50x, 1077 \text{ cm}^{-1}) = \frac{N_{\text{bulk}} I_{\text{poly}}}{N_{\text{poly}} I_{\text{bulk}}}, \quad (1)$$

where I_{bulk} and I_{poly} are measured intensities of the bulk compound and the metalized polymer substrate respectively. N_{bulk} and N_{poly} are the number of molecules in the bulk and adsorbed on metalized polymer substrate, respectively. For a consistent sample to sample intensity reference the 521 cm^{-1} phonon peak of a clean silicon wafer was used to provide a basis for normalization of the spectra. For a Raman $\nu_{\text{C-F}}$ intensity reference, the Raman peak from the spectrum of pure FBT was used.²⁴ Given the liquid density of FBT as 1.197 g/cm^3 , approximately 4.6×10^9 molecules should

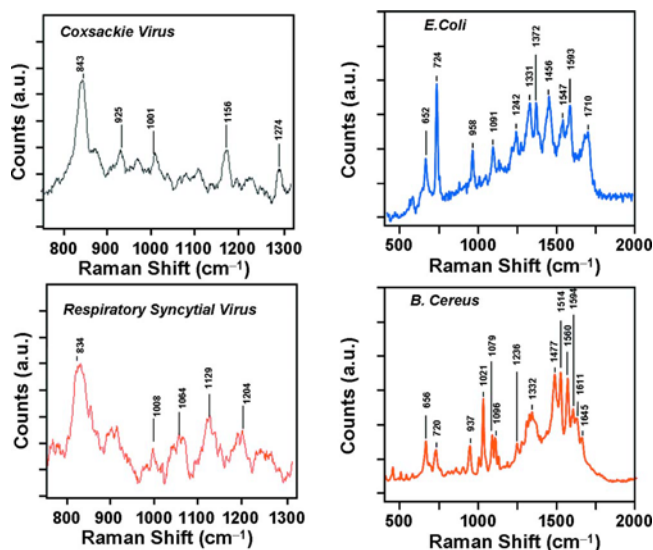


FIG. 3. (Color online) SERS spectra of single entities of Coxsackievirus (nonenveloped virus), respiratory syncytial virus (enveloped virus), *E. coli* (gram-negative bacteria), and *B. cereus* (gram-positive bacteria) adsorbed onto 60 nm Ag metalized PPX-Cl substrates.

contribute to the SERS signal (N_{bulk}) as derived from the volume in the focal region of our confocal optics. The number of molecules (N_{poly}) is estimated for practical purposes as 3.6×10^6 based on a 1 μm diameter laser spot the circular geometric area of the sample surface within the beam. Approximately $I_{\text{poly}}/I_{\text{bulk}}$ equals to 550 (e.g., $I_{\text{bulk}}=51\,336$ counts $I_{\text{poly}}=28\,092\,053$ counts for 10 s accumulation). On this basis a practical enhancement factor for the 60 nm Ag metalized film is $\sim 1 \times 10^6$. The actual number of molecules on the surface would be greater depending on the actual area of the metal film. Estimates from Brunauer-Emmet-Teller measurements with quartz crystal microbalance techniques indicate actual surface areas ~ 10 – 100 times greater than the geometric (more exact measurements will be reported elsewhere). In any case, the enhancement for our surfaces is amply sufficient to allow good quality spectra for quantitative measurements.

B. SERS measurements for pathogens

E. coli (gram-negative bacteria), *B. cereus* (gram-positive bacteria), *Coxsackievirus* (nonenveloped virus), and *respiratory syncytial virus* (enveloped virus) were selected as test organisms for our initial assessment of the nanostructured SERS substrate application for pathogen detection. Figure 3 shows the SERS spectra of *single E. coli*, *B. cereus*, *Coxsackievirus*, and *RSV* pathogen particles on the nanostructured silver substrates. Spectra were collected at 2.5 mW laser power, 632 nm wavelength, and a 10 s collection time.

These spectra reveal that the bio-organisms were captured as an integral species with no significant degradation, as shown by reasonable assignments of the vibrational features based on standard empirical peak correlations. Typical Raman bands of proteins, phospholipids, and polysaccharides can be observed in the *E. coli* and *B. cereus* bacteria spectra

TABLE I. SERS peak assignments for pathogens investigated in this study.

Assignment	SERS shifts (cm^{-1})			
	<i>E. coli</i>	<i>B. cereus</i>	<i>Respiratory syncytial virus</i>	<i>Coxsackie virus</i>
Guanine, tyrosine (nucleic acid)	653	656	...	686
Adenine	724	720	...	724
Tyrosine	837	842
C=C deformation	958	937	...	925
Phenylalanine	1004	1002
C-C stretching (phospholipids or carbohydrates)	...	1022
C-N stretching (glycoprotein)	1064	...
Carbohydrates (C-C stretching, C-O-C stretching)	1091	1096
C-C stretching (protein)	1130	1156
Tyrosine	1204	...
Thymine	1272
Amide III (random)	1242	1236
CH deformation	1330	1332
COO stretching	1372	...	1320	1337
CH ₂ deformation	1456	1477	1480	1437
Amide II	...	1559
Adenine, guanine (ring stretching)	1593	1594	1610	1603
Amide I	1710	1650

(Table I) and spectra match well with literature.^{27–29} The band at 653 cm^{-1} is most likely from guanine and tyrosine. The strong band at 724 cm^{-1} is likely from polysaccharides and adenine while that 958 cm^{-1} is likely from C=C deformation. The band at 1091 cm^{-1} correlates with those expected from carbohydrates (mainly from C-C stretching, C-O-C stretching of 1,4-glycosidic link may also contribute to the peaks). For *E. coli*, the peak at 1710 cm^{-1} can be associated with the C=O of an ester group. The amide I (C=O stretching and C-N-H deformation) bands, which are the characterizations of protein backbones, can be assigned to peaks in the vicinity of 1650 and 1240 cm^{-1} , respectively. The band at 1372 cm^{-1} is most likely from COO^- stretching. The band at 1456 cm^{-1} is expected for CH_2 deformation. The band at 1593 cm^{-1} correlates with adenine and guanine (ring stretching). For *RSV*, the SERS bands at ~ 830 and 1005 cm^{-1} are presumed to be from tyrosine and phenylalanine, respectively,³⁰ while those at ~ 1060 and $\sim 1130 \text{ cm}^{-1}$ can be ascribed to C-N stretching and C-C stretching, respectively.³¹ Tyrosine is also supposed to show Raman features at $\sim 1200 \text{ cm}^{-1}$. For *Coxsackievirus*, the SERS band at 688 cm^{-1} is assigned to guanine and tyrosine. Other major SERS bands present at 724 , 843 , 925 , 1001 , 1156 , and 1274 cm^{-1} , are most likely from adenine, tyrosine, C=C deformation, phenylalanine, C-C stretching (protein), and thymine, respectively. In all cases the peaks fit with expected features for the organisms. Further work is needed in order to find deeper correlations with the exact details of the attachment point of the organism on the SERS surface and the appearance of various constituent groups located in different regions of the organism.

C. SERS results on reproducibility of the fingerprint spectra

Figures 4(a) and 4(b) show the reproducibility of SERS spectra of single *E. coli* and *RSV* pathogen particles on the

nanostructured silver substrates, respectively. Figures 4(c) and 4(d) show optical microscope images of the samples. Both data were collected at 2.5 mW laser power and 632 nm wavelength with a 10 s collection time. The *E. coli* data were collected by first identifying the location of a bacteria particle ($\sim 1 \mu\text{m}$ size) by optical microscope imaging on the substrate [Fig. 4(c)] with the images taken randomly with wide distances between ($\geq 1 \mu\text{m}$) bacterial particle. The *RSV* data were collected using an automated surface scan to statistically find a particle within the image field since the pathogens were of too small a size to readily identify their

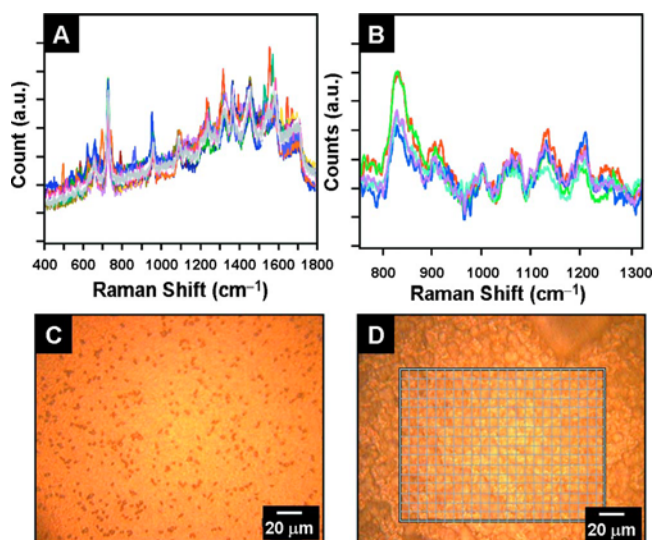


FIG. 4. (Color online) Sets of superimposed (a) *E. coli* and (b) *RSV* SERS spectra collected from nanostructured PPX films coated with a thin 60 nm Ag layer. The variation of the *E. coli* spectra on the silver SERS substrate was obtained from 20 individual cells. The peak at the 1372 cm^{-1} shows a relative deviation of 15%. The variation of the *RSV* spectra on the silver SERS substrate was obtained from six individual particles. Optical images of surface for the bacteria and virus are shown in (c) and (d), respectively.

location. Again, wide variations in the sampling distances were used. The data show highly reproducible spectra across a surface with a relative deviation of 15% for the *E. coli* spectra with 20 samples; the RSV spectra were similarly reproducible, though only six particles were analyzed. Preliminary data (to be published) show that the high reproducibility is also maintained from substrate to substrate with careful control of preparation and bio-organism capture.

In order to check the reproducibility of the Ag/PPX-Cl films relative to standard Ag island films on glass, samples of the latter substrates were prepared with identical vapor deposition of Ag films on clean glass slide substrates and *E. coli* bacteria were collected on the substrates using the identical procedures as for the Ag/PPX-Cl substrates. After many trials, in our hands it was clear that while excellent EFs were obtained, the Ag islands were highly unstable in an unpredictable way to the collection process. This led to irreproducible SERS spectra for the bacteria particles across the surfaces, often with well over orders of magnitude variations in the signal intensities and with significant shifts in the relative fingerprint peak intensities (data not shown).

Finally, we note that we have carried out preliminary experiments, done under the same controlled conditions, using Au metalized PPX-Cl substrates and find similar high reproducibility of the SERS spectra with useful EFs. In the case of the Au films the EFs can be several times to an order of magnitude lower than for the Ag films but the Au films are extremely stable and show the ability to be cleaned and repeatedly reused. These results will be reported elsewhere.

IV. CONCLUSIONS

The results of this study show that Ag metalized PPX-Cl substrates, designed specifically with controlled metal film morphologies embedded within the nanostructured columnar features of the polymer substrates, can provide highly sensitive pathogen detections for test organisms (e.g., *E. coli*, *B. cereus*, *Coxsackievirus*, and *RSV*) with high sample to sample reproducibility (15% variation between particles) while providing a surface with the capability of sustaining the integral structure of biospecies. The advantage of these new types of substrates is that no template or lithography is involved, thus providing a simple, inexpensive, and quick production method to achieve highly sensitive and spatially uniform SERS substrates. The vibrational spectrum obtained from the SERS displays fingerprinting information of the chemical composition from the membrane of the pathogen. Typical Raman bands of proteins, phospholipids, and polysaccharides can be observed in the spectrum. While the data show that local plasmon excitations provide high SERS signal intensities associated with an integral organism, the specific interactions that bind the organism to the active SERS *hot spots* and the exact details of the chemical constituents presented within the SERS excitation volume remain uncertain. Further work is required to provide these important details of the organism-substrate interface and such work is in progress in our laboratories, including other spectroscopies as well as the use of highly controlled, inter-

vening molecular functionalization of the SERS substrate to produce new organism-metal interphases.

There are substantial needs for the high performance SERS substrates in research laboratories and different industrial settings. Existing diagnostic procedures to identify pathogens are costly, time consuming, and may not be available in medically underserved populations. Low cost and highly sensitive SERS substrates will mark an important advancement in diagnostic methods. The ability to treat infections effectively will be improved by rapid accurate identification of the etiological agents. Rapid diagnostic methods such as SERS will greatly improve surveillance for emerging virus infections (such as SARS-CoV or influenza). The use of "fingerprint" identification of agents is an enabling technology designed to handle mixtures of agents, and to operate in the presence of common interferents. To a good extent, the current data in our study show that this looks promising since there are a number of spectral features in a given bio-agent fingerprint and with careful spectral analysis a wide variety of analytes in principle could be distinguished from one another in mixtures. Rapid data analyses can be performed in seconds to determine the specific species of the bioagents and a display of the detailed threat of this or these agents. Innovation in reliable, inexpensive diagnostics, such as novel SERS substrate, can bring technological advancements to populations where the need is great.

ACKNOWLEDGMENTS

This research was supported by a Young Investigator Program Award (to M.C.D) from the Office of Naval Research (Grant No. N000140710801), a seed grant from the Huck Institute Life Sciences at Penn State and partial support from the NSF funded PSU Center for Nanoscale Science (Grant No. MRSEC DMR-0080019) and DTRA.

- ¹P. Yager, G. J. Domingo, and J. Gerdes, *Annu. Rev. Biomed. Eng.* **10**, 107 (2008).
- ²J. Kneipp, H. Kneipp, and K. Kneipp, *Chem. Soc. Rev.* **37**, 1052 (2008).
- ³P. L. Stiles, J. A. Dieringer, N. C. Shah, and R. R. Van Duyne, *Annu. Rev. Anal. Chem.* **1**, 601 (2008).
- ⁴K. A. Hartman, N. Clayton, and G. J. Thomas, *Biochem. Biophys. Res. Commun.* **50**, 942 (1973).
- ⁵M. G. Albrecht and J. A. Creighton, *J. Am. Chem. Soc.* **99**, 5215 (1977).
- ⁶D. L. Jeanmaire and R. P. Van Duyne, *J. Electroanal. Chem.* **84**, 1 (1977).
- ⁷M. Moskovits, L. L. Tay, J. Yang, and T. Haslett, *Optical Properties of Nanostructured Random Media* (Springer-Verlag, Berlin, Germany, 2002), Vol. 82, p. 215.
- ⁸A. M. Stacy and R. P. Van Duyne, *Chem. Phys. Lett.* **102**, 365 (1983).
- ⁹I. Pockrand, *Surface Enhanced Raman Vibrational Studies at Solid/Gas Interfaces* (Springer, Berlin, 1984).
- ¹⁰U. Kreibig, B. Schmitz, and H. D. Breuer, *Phys. Rev. B* **36**, 5027 (1987).
- ¹¹K. Kneipp, H. Kneipp, V. B. Kartha, R. Manoharan, G. Deinum, I. Itzkan, R. R. Dasari, and M. S. Feld, *Phys. Rev. E* **57**, R6281 (1998).
- ¹²S. Farquharson, L. Grigely, V. Khitrov, W. Smith, J. F. Sperry, and G. Fenerty, *J. Raman Spectrosc.* **35**, 82 (2004).
- ¹³N. Peica, I. Pavel, S. C. Pinzaru, V. K. Rastogi, and W. Kiefer, *J. Raman Spectrosc.* **36**, 657 (2005).
- ¹⁴M. Kahraman, M. M. Yazici, F. Sahin, O. F. Bayrak, and M. Culha, *Appl. Spectrosc.* **61**, 479 (2007).
- ¹⁵P. F. Liao, J. G. Bergman, D. S. Chemla, A. Wokaun, J. Melngailis, A. M. Hawryluk, and N. P. Economou, *Chem. Phys. Lett.* **82**, 355 (1981).
- ¹⁶N. Felidj, J. Aubard, G. Levi, J. R. Krenn, M. Salerno, G. Schider, B. Lamprecht, A. Leitner, and F. R. Aussenegg, *Phys. Rev. B* **66**, 245407

- (2002).
- ¹⁷C. L. Haynes and R. P. Van Duyne, *J. Phys. Chem. B* **105**, 5599 (2001).
- ¹⁸M. D. Musick, C. D. Keating, L. A. Lyon, S. L. Botsko, D. J. Pena, W. D. Holliday, T. M. McEvoy, J. N. Richardson, and M. J. Natan, *Chem. Mater.* **12**, 2869 (2000).
- ¹⁹R. A. Tripp, R. A. Dluhy, and Y. P. Zhao, *Nanotoday* **3**, 31 (2008).
- ²⁰M. C. Demirel, *Colloids Surf., A* **321**, 121 (2008).
- ²¹M. C. Demirel, M. Cetinkaya, A. Singh, and W. J. Dressick, *Adv. Mater. (Weinheim, Ger.)* **19**, 4495 (2007).
- ²²S. Boduroglu, M. Cetinkaya, W. J. Dressick, A. Singh, and M. C. Demirel, *Langmuir* **23**, 11391 (2007).
- ²³A. Cetinkaya, S. Boduroglu, and M. C. Demirel, *Polymer* **48**, 4130 (2007).
- ²⁴P. Kao, N. Malvadkar, H. Wang, D. L. Allara, and M. C. Demirel, *Adv. Mater. (Weinheim, Ger.)* **20**, 3562 (2008).
- ²⁵M. Cetinkaya, N. Malvadkar, and M. C. Demirel, *J. Polym. Sci., Part B: Polym. Phys.* **46**, 640 (2008).
- ²⁶G. Mie, *Ann. Phys.* **25**, 377 (1908).
- ²⁷W. R. PremaSiri, D. T. Moir, M. S. Klemperer, N. Krieger, G. Jones, and L. D. Ziegler, *J. Phys. Chem. B* **109**, 312 (2005).
- ²⁸R. M. Jarvis and R. Goodacre, *Anal. Chem.* **76**, 40 (2004).
- ²⁹K. C. Schuster, I. Reese, E. Urlaub, J. R. Gapes, and B. Lendl, *Anal. Chem.* **72**, 5529 (2000).
- ³⁰P. D. Bao, T. Q. Huang, X. M. Liu, and T. Q. Wu, *J. Raman Spectrosc.* **32**, 227 (2001).
- ³¹S. Shanmukh, L. Jones, J. Driskell, Y. P. Zhao, R. Dluhy, and R. A. Tripp, *Nano Lett.* **6**, 2630 (2006).